Journal Name

ARTICLE

Isomer and Conformer Selective Atmospheric Pressure Chemical Ionisation of dimethyl phthalate

Received 00th January 20xx,
Accepted 00th January 20xx

DOI: 10.1039/x0xx00000x

www.rsc.org/

Bartosz Michalczuk[ab], Ladislav Moravský [a], Peter Papp[a], Pavel Mach[c], Martin Sabo[a] and Štefan Matejčík *[a]

In this work we have studied ionisation mechanism of Atmospheric Pressure Chemical Ionisation (ACPI) for three isomers of dimethyl phthalate (dimethyl phthalate –DMP (ortho - isomer), dimethyl isophthalate – DMIP (meta) and dimethyl terephthalate – DMTP (para)) using Ion Mobility Spectrometry (IMS) and IMS combined with orthogonal acceleration Time of Flight Mass Spectrometer (oa-TOF MS). The molecules were chemically ionised by reactant ions $H^+\cdot(H_2O)_n$ (n=3 and 4). The positive IMS and IMS-oaTOF mass spectra of isomers showed significant differences in the ion mobilities and in the ion composition. The IMS – oaTOF spectra consisted of clusters ions $M\cdot H^+\cdot(H_2O)_n$ with different degree of hydration (n=0,1,2,3) for different isomers. In the case of DMP isomer we have observed almost exclusive formation of $M\cdot H^+$ by proton transfer ionisation, while in case of DMIP and DMTP hydrated ions $M\cdot H^+\cdot(H_2O)_n$ (n=1,2,3) respectively $M\cdot H^+\cdot(H_2O)_n$ (n=0,1,2) were detected, formed via adduct formation reaction. This behaviour was elucidated by differences in ionisation processes. In order to elucidate the ionisation processes we have carried out DFT calculations of the structures and energies of the neutral and protonated and hydrated isomers (for different conformers) and calculated corresponding proton affinities (PA) and hydration enegries.

Introduction

Phthalates, also known as phthalate esters, is a group of chemicals which is widely used in consumer products like children's toys, building materials, pharmaceuticals, furnishing, cosmetics, food packaging and many others. Phthalates are also used as plasticizers in rigid polymers like polyvinyl chloride or other polymers [1]. It is worth to note that their content can make up to 50% of the final product weight [2]. The problem is that phthalates are produced in large quantities and can be easily released from plastics and contaminate soil or water [3]. The presence of phthalates in the environment can be a threat to nature and to human health. The fact that esters of phthalic acid are thought to be endocrine disruptors, [4,5] requires development of a suitable analytical methods for their detection in samples with very low concentrations and considering economic aspects.

In recent years, the problem related to the omnipresence of phthalates has been spotted. That fact is reflected by dozens of scientific reports published recently [6,7,8]. Different analytical techniques have been involved in the investigation of phthalates. For instance, high performance liquid chromatography (HPLC) or gas chromatography - mass spectrometry (GC-MS) were used to determinate phthalates in industrial emissions and food samples [9,10]. Hyphenation techniques, including HPLC–atmospheric pressure chemical ionization tandem mass spectrometry system (HPLC–APCI-MS/MS), [11] Liquid Chromatography–Atmospheric Pressure Chemical Ionization–Mass Spectrometry (LC-APCI-MS) [12] are usually applied to study isomeric species. GC or HPLC have advantages such as well-developed databases of compounds or the versatility of these methods, but as every analytical method, they have also disadvantages. The main obstacle is a special preparation method for the samples before the analysis and the relatively long time of the analysis [13].

The ion mobility spectrometry has some advantages which make this technique suitable to detect these types of compounds. IMS is a spectrometric method with fast response, i.e., fractions of a second after introducing the sample to the device. The high sensitivity allows detection at very low concentration (down to ppt for some compounds). In many cases, the sample can be investigated as delivered, without additional purification or pre-concentration. The first application of the IMS technique for detection of phthalates was by Hagen, [14] who demonstrated among others the detection of the dimethyl phthalate isomers by IMS in positive and negative polarity. The detection of dimethyl phthalates in negative polarity IMS was reported by Poziomek et al., [15] who used IMS for detection of different phthalates esters in water. Barnet et al.[16] applied in negative polarity the field asymmetric IMS (FAIMS) combined with mass spectrometer and electrospray ionization (ESI) ion source to separate three

[a] Department of Experimental Physics, Comenius University, Mlynská dolina F2, 84248 Bratislava, Slovakia.
[b] Department of Chemistry, Siedlce University, 3 Maja 54, 08-110 Siedlce, Poland.
[c] Department of Nuclear Physics and Biophysics, Comenius University, Mlynská dolina F1, 84248 Bratislava, Slovakia.

isomers of phthalic acid. Midey et al. [17] presented results where high-performance ion mobility spectrometry with direct electrospray ionization (ESI-HPIMS) was used to detect several additives and contaminants in food, including phthalates.

In this work we present a study focused on detection of the isomers of DMP in positive polarity IMS in combination with APCI ion source based on corona discharge of dehumidified ambient air. We have observed significant differences in IMS spectra of the isomers, larger as expected from the geometry differences of the isomers. For this reason, we have studied the mechanism of the separation in more detail using the IMS-oaTOF instrument. This study revealed that the APCI of DMP isomers results in formation of protonated ions with different degree of hydration.

Table 1. Structures, vapor pressures for all investigated phthalates as determined in present IMS experiment.

Isomer		Vapour pressure (298K) [18]
DMP	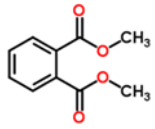	0.304 Pa
DMIP	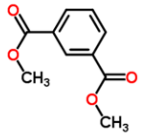	0.099 Pa
DMTP	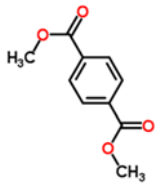	0.01 Pa

Experimental

IMS-oaTOF instrument

The IMS-oaTOF MS instrument used in this work is a homemade IMS instrument with APCI ionisation source based on corona discharge (CD). The spectrometer has been described in detail elsewhere[19,20,21]. The IMS was operated in positive polarity and at sub-atmospheric pressure (700 mbar). This offers simple sampling of volatile organic compounds by the capillary inlet. All operating parameters are summarized in Table 2. The sample flow rate was controlled by a micro-splitter valve and adjusted by a flow meter (20 ml/min). The ion mobility scale was calibrated using 2,6-di-tert-butylpyridine (Sigma-Aldrich) as a standard compound with the well-known reduced mobility of 1.42 $cm^2V^{-1}s^{-1}$[22].

The hybrid IMS-oaTOF instrument can be operated in three working modes: i) the IMS mode in which IMS spectra are recorded, ii) the TOF mode with opened IMS ion gate and continuous transport of ions through the IMS to record TOF mass spectra and iii) third mode, the IMS and TOF gates are operated synchronously leading to two dimensional IMS-MS spectra. In this mode we are able to assign IMS peaks to ions with a particular m/z.

Gases and chemicals

As a drift gas in IMS, we used zero air generated by a MaSa Tech zero air generator and an additional moisture trap (Agilent) resulting in water concentration of ~20 ppm. In case of sample flow, non-purified lab air was constantly sucked in, while the IMS was operated in sub-atmospheric pressure. The sample flow rate was controlled by a micro-splitter valve (Supelco) accompanied by a capillary and a gas flow meter (Platon). The phthalates were supplied from Sigma-Aldrich with the following purities: dimethyl isophthalate 99%, dimethyl phthalate 99%, dimethyl terephthalate 99%.

The vapours of the phthalates were introduced into the reaction region of the IMS through a sample inlet. The phthalates were placed in a glass syringe (about 0.5 g) and we waited at least 30 min to achieve an equilibrium between the gas and the solid or liquid phase. Afterwards, the syringe was connected via a capillary with the sample inlet and using a syringe pump (Kent Scientific), the sample was introduced into the reaction region of the IMS with a pre-set flow rate.

Table 2. Parameters of IMS used in the experiment.

Operating Parameters	
IMS drift tube length	12.05 cm
Electric field intensity	665.5 $V.cm^{-1}$
IMS operating pressure	700 mbar
IMS operating temperature	345 K
Drift gas flow	400 sccm
Sample gas flow	20 sccm
CD current	10 µA
Shutter grid pulse width	60 µs
Shutter grid frequency	16 Hz

Results and discussion.

We have ionised the phthalates using atmospheric pressure chemical ionisation (APCI) by reactant ions (RI) formed in the corona discharge in the dehumidified ambient air. The ambient air used as a drift gas in IMS and feed gas in APCI was processed by system of filters and moisture traps reducing the water concentration to ~ 20 ppm level. The positive corona discharge

in this gas and at the temperature of 345 K resulted in generation of Reactant Ions (RI) $H^+\cdot(H_2O)_n$ (n=3,4) and small amount of $NH_4^+(H_2O)_n$ (n=0,1), as established by the IMS-oaTOF MS. The $H^+\cdot(H_2O)_{3,4}$ ions were dominant RI, therefore, we are going to concentrate on the processes associated with these ions. The APCI ionisation of phthalates in the IMS-oaTOF MS instrument includes the following reactions of the RI with the analyte:

$$H^+\cdot(H_2O)_n + M \rightarrow M\cdot H^+ + (H_2O)_n \quad (1)$$

$$\rightarrow [M\cdot H^+\cdot(H_2O)_n]^{\#} \rightarrow$$

$$\rightarrow M\cdot H^+\cdot(H_2O)_m + (H_2O)_{n-m} \quad (2)$$

Where M represents an isomer of dimethyl phthalate, n=3 and 4, and m=1, 2 and 3. The proton transfer reaction (1) is very efficient two body reaction with rate coefficient close to the collision rate if the proton affinity of the molecule PA(M) exceeds the proton affinity of the corresponding $(H_2O)_n$ cluster ($PA((H_2O)_{3,4})$)[24]. The adduct ion formation reactions (2), depends on the bond energy between protonated water clusters to molecule M - $H^+\cdot(H_2O)_m$ (m=1,2) and the bond energy of the water to the ion $MH^+\cdot(H_2O)_{m-1}$-(H_2O).

Figure 1 shows the positive IMS spectra of the ambient air (RI spectrum) and of the DMP isomers. In the RI spectrum we see the reactant ion peaks with the reduced ion mobilities K_0 of 2.22 $cm^2V^{-1}s^{-1}$ ($NH_4^+\cdot(H_2O)_{0,1}$), 2.09 $cm^2V^{-1}s^{-1}$ $H^+\cdot(H_2O)_n$ (n=3,4) and weak ion peaks with K_0 ~ 1.90 and 1.10 $cm^2V^{-1}s^{-1}$ which we associate with the trace impurities originating from the laboratory air. The spectra formed upon APCI of DMP, DMIP and DMTP show additional IMS peaks of 1.57 $cm^2V^{-1}s^{-1}$, 1.36 $cm^2V^{-1}s^{-1}$ and 1.40 $cm^2V^{-1}s^{-1}$ respectively. The vapours of the DMP isomers were diluted to prevent saturation and removal of all RI. The displayed spectra were measured at relative low concentrations for this reason molecular dimer ions peaks were observed only for the DMIP molecule, which has a stronger affinity to dimerise. The present IMS spectra are in qualitative agreement with the observation of Hagen[14] who in the positive polarity observed significant differences in reduced ion mobilities of DMP (1.54 $cm^2V^{-1}s^{-1}$) on one side and DMIP and DMTP (1.45 respectively 1.47 $cm^2V^{-1}s^{-1}$) on the other. However, we would like to note, that present data were recorded under substantially different experimental conditions, the main difference was the drift gas (nitrogen in case of Hagen, air in present) and the drift gas temperature. In present experiment the temperature was 345 K, while Hagens experiments were carried out at high temperature of 503 K. High temperature influence the hydration of the RI and naturally also the ionisation process. Nevertheless, the spectra have similar character.

From IMS spectra alone it is not possible to determine the m/z of the ions travelling under single IMS peak. The two-dimensional IMS-oaTOF MS spectra allowed us to assign m/z to the IMS peaks (Figure 2). The x-axis represents the time of flight of the ions in the TOF MS. In the Figure 2 we indicate m/z and the corresponding formula of the ions. The y-axis represents the drift time of the ions in the IMS, which corresponds to the ion mobility. The resolving power of IMS in IMS-oaTOF instrument was lower than in the standalone IMS instrument. Based on these spectra we were able to assign m/z to the IMS peaks and the structural formula of the ions.

In the case of DMP (Fig. 2a) the monomer peak of K_0=1.57 $cm^2V^{-1}s^{-1}$ consisted of $M\cdot H^+$ (m/z 195), while the weak IMS peak of K_0=1.38 $cm^2V^{-1}s^{-1}$ was identified as $M\cdot H^+\cdot(H_2O)$ (m/z 213) with lower ion mobility of ~1.36 $cm^2V^{-1}s^{-1}$. At higher concentrations of DMP (not presented in Fig. 2a) we were able to detect also dimers $M_2\cdot H^+$ (m/z 389) and $M_2\cdot H^+\cdot(H_2O)$ (m/z 407). The spectrum of DMIP (Fig. 2b) shows a completely different pattern. The monomer IMS peak has significantly lower ion mobility compared to DMP and consists of $M\cdot H^+\cdot(H_2O)_n$ (n=0, 1,2, m/z 195, 213and 231). The protonated ion $M\cdot H^+$ was very weak (invisible in 2D spectra). At higher concentration we detected the dimer ions including $M_2\cdot H^+$ (m/z 389), $M_2\cdot H^+\cdot(H_2O)$ (m/z 407)

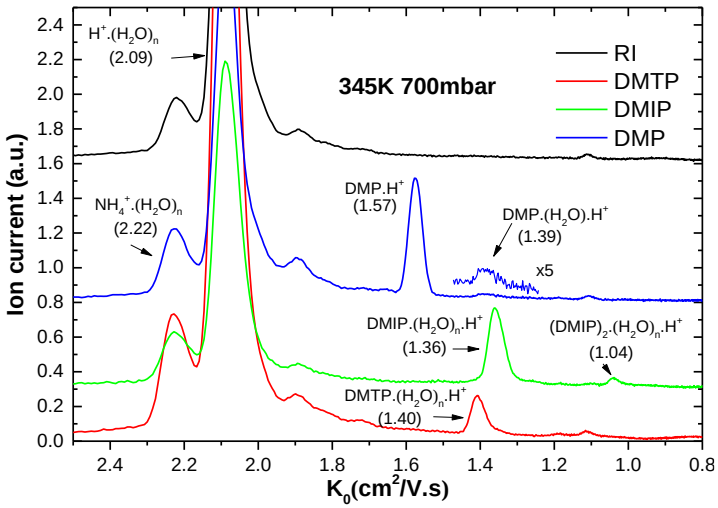

Figure 1. IMS spectrum of DMP isomers at temperature 345 K and gas pressure 700 mbar.

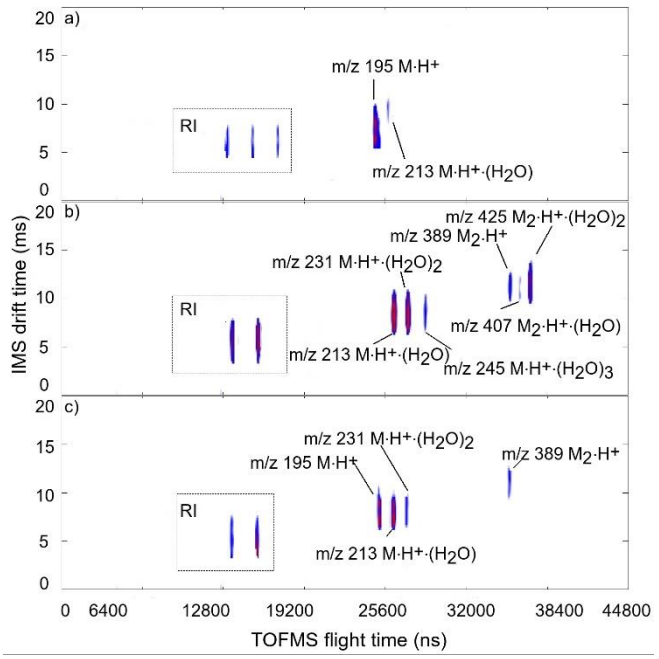

Figure 2. IMS-MS spectra of the phthalate ions formed via APCI a) DMP, b) DMIP, c) DMTP.

and the strongest ion present in the spectrum $M_2{\cdot}H^+{\cdot}$ $(H_2O)_2$ (m/z 425).

In the spectrum of DMTP the monomer IMS peak consisted of three ions $M{\cdot}H^+{\cdot}(H_2O)_n$ (n=0,1,2, m/z 195, 213 and 231). At higher concentrations, we have registered also a weak dimer ion $M_2{\cdot}H^+$ (m/z 389). The reduced ion mobilities of monomer and dimer IMS peaks we have summarized in the Table 3.

Table 3. Detected ions and their reduced mobilities K_0

Molecule	Monomer ions	K_0 $cm^2V^{-1}s^{-1}$	Dimer ions	K_0 $cm^2V^{-1}s^{-1}$
DMP	$M{\cdot}H^+$ (95%)	1.57	$M_2{\cdot}H^+{\cdot}(H_2O)_n$	1.04
	$M{\cdot}H^+{\cdot}(H_2O)$ (<5%)	1.38	n=0,1	
DMIP	$M{\cdot}H^+{\cdot}(H_2O)_n$ n=1,2,3	1.36	$M_2\,H^+{\cdot}(H_2O)_n$ n=0,1,2	1.04
DMTP	$M{\cdot}H^+{\cdot}(H_2O)_n$ n=0,1,2	1.40	$M_2\,H^+{\cdot}(H_2O)_n$ n=0	1.04

The Figure 2 demonstrates, that the monomer peaks in IMS spectra consist of the ions $M{\cdot}H^+{\cdot}(H_2O)_n$ (n=0,1,2,3). As discussed already two different reaction mechanism are responsible for the ionisation, the reaction (1) and (2). In the case of DMP, the ionisation of conformer with high proton affinity DMP(III) (see supplementary material for details regarding conformers) results in the formation of $DMP.H^+$ ion via proton transfer reaction (1), which appears in IMS spectrum with K_0=1.57 $cm^2V^{-1}s^{-1}$. The present calculations (Table 5) indicate, that this ion interacts weakly with the water molecules and does not form hydrated ions. The second, weak peak of DMP at K_0=1.38 $cm^2V^{-1}s^{-1}$ was formed via reaction (2) with other conformers of DMP with lower PA. This ion we have assigned to $M{\cdot}H^+{\cdot}(H_2O)$.

In the case of DMIP and DMTP isomers, we have detected only hydrated ions $M{\cdot}H^+{\cdot}(H_2O)_n$ (n=1,2,3 for DMIP and n=0,1,2 for DMTP). These ions were formed via reaction (2), as the reaction (1) is for these isomers endothermic and therefore slow. The present calculations show that the protons in these ions are bound to water, forming hydronium ions H_3O^+ and that the hydronium ion interacts with the molecules. The ions travel along the drift tube and establish equilibrium distribution regarding the degree of hydration. The differences in the hydration of the isomers DMIP and DMTP can be explained by the differences in the bond energies of water to the $M{\cdot}H^+(H_2O)$ ions (Table 5).

The above-mentioned interpretation of the experimental data was supported by the calculations of the structure and energetics of the DMP isomers, their protonated and hydrated ions.

Table 4. Proton affinities of DMP isomers, calculated using different methods and compared with the values of PA found in the literature.

Molecule	M06-2X (eV)	ωB97X-D (eV)	Literature (eV)
DMP	9.76	9.70	-
DMIP	8.80	8.77	8.74[24]
DMTP	8.60	8.74	8.74[24]
H_2O		7.16	
$(H_2O)_2$		8.56	
$(H_2O)_3$		9.07	9.26[23]/9.32[30]
$(H_2O)_4$		9.37	9.70[23]/9.64[30]

The values of PA's are important for evaluation of the probability of the proton transfer reactions (1). In the literature we have found only experimental values for DMIP and DMTP [24]. For this reason, we have calculated the PA of DMP and its isomers using quantum chemistry methods. We have carried out density functional theory [25] (DFT) calculations of the PA of DMP, DMIP, DMTP, water clusters and the combined phthalate water clusters. As the initial step the M06-2X [26,27] functional was used to identify the ground state geometries and energies of all three studied phthalates, their neutral and protonated counterparts. We have considered three conformers for DMP, three for DMIP and two for DMTP. The attachment of the proton was considered to take place on the nonbonding electron pair of carboxylic oxygens. This led to four protonated DMP conformers, four protonated DMIP and two protonated DMTP conformers. Although the energetically lowest neutral conformer was DMIP(II), the differences from the other conformers are very small at this level of theory. The five DMIP and DMTP conformers differed only by 0.014 eV while the energies of DMP conformers were hundreds of meV above the DMIP(II), up to 0.315 eV. The single point recomputed energies with MP2 changed the relative order of conformers to DMTP(II) to be the lowest, however the differences remained still in the order of tenths and in case of DMP hundreds of meV only (please see Table S.1 and S.2 in supplementary material). Among all the protonated structures the M06-2X energetically lowest $H^+{\cdot}$DMP(III) was lower by more than several hundreds of meV from the other 9 structures, which is in excellent agreement with the single point MP2 results.

Table 4 summarizes the calculated proton affinities obtained with M06-2X/6-311G(2df,2pd) and ωB97X-D/6-311+G(2d,p)[28,29]. Both functionals were pointed out by Burns et al. [28] as the best for noncovalent interactions, hydrogen bonding systems; the first for short and medium range distances (below 5 Å) while the second for long-range distances as well. Moreover, they have shown that the mean errors of these methods with the choice of triple zetta basis set will be around 0.1 eV and below. According to present results the DMP isomer has the highest proton affinity (its conformer DMP(III), for more details see the supplementary material), in comparison the PAs of DMIP and DMTP conformers are ~1 eV lower. In the case of DMIP and DMTP the current PA values are in reasonable agreement with the experimental values of PA. [24]
The PA's of DMP isomers we can compare with the PA's of the water clusters (RI precursors), which depend strongly on the size of the clusters. In the present case the RI consist of $H^+\cdot(H_2O)_n$ (n=3,4) with a proton binding energy of 9.32 and 9.64 eV, respectively[30]. The size and distribution of RI generated in APCI depends on the temperature and concentration of water[31] and the size distribution of the RI allows determination of the water concentration of the gas.

Table 5. Theoretical values of reaction enthalpies for the hydration of the protonated ions calculated at ωB97X-D/6-311+G(2d,p) level.

Products	M = DMP	M = DMIP	M = DMTP	M = H_2O
$M^+\cdot H^+ + H_2O$	0.36	0.91	0.82	1.58
$M + H_3O^+$	2.90	1.59	2.40	1.58
$M\cdot H^+ + (H_2O)_2$	0.54	1.61	1.23	2.35
$M\cdot H_3O^+ + H_2O$	0.37	0.89	0.59	0.97
$M\cdot H^+ + (H_2O)_3$	0.85	1.78	1.61	2.72
$M\cdot H_3O^+ + (H_2O)_2$	0.66	1.31	1.24	1.58
$M\cdot H^+ + (H_2O)_4$	0.62	1.74	1.72	2.77
$M\cdot H_3O^+ + (H_2O)_3$	0.77	1.21	1.41	1.70

The ωB97X-D was used to model the protonated phthalate water clusters, up to 4 waters attached to DMP, DMIP and DMTP molecules and ions. Some of the interaction energies of $M\cdot H^+$ with $(H_2O)_{1\text{-}4}$ and $M\cdot H_3O^+$ with $(H_2O)_{1\text{-}3}$ are listed in the Table 5, more reactions and figures of different geometries can be found in the supplementary materials. The DMP isomer has the highest PA and the hydration energies are lower in comparison to DMIP and DMTP and of $(H_2O)_n$. The latter two isomers have very similar hydration energies, however, in case of DMTP $M\cdot H^+$ hydration energies are systematically lower compare to DMIP. This picture was supported by the calculated geometries of the ions. In the case of DMP the proton is attached to molecule in all $(H_2O)_{1\text{-}4}$ clusters. In contrast DMIP accepts the proton only with one water molecule in cluster (H_3O^+), the larger hydrated clusters of DMIP are caring the proton on the water molecules as well. Finally, the DMTP accept the proton with up to two water molecules. This is obvious from the calculated $M\cdot H^+\text{-}(H_2O)_n$ interaction energies, which are lower for the DMTP than for the DMIP at the same level of hydration.
The PA's of RI exceed the PA's of most DMP and all DMIP and DMTP conformers and for this reason, the proton transfer reactions (1) for these two isomers are absent. In the case of DMP, exclusively the conformer DMP(III) has PA exceeding the proton bond energy of RI and the proton transfer reaction occurs. The present calculations and the experimental results indicate, that in case of conformer DMP(III) the ionisation is conformer selective and leading to formation of protonated ion $M\cdot H^+$. The calculations also indicate this protonated ion doesn't react with water and we did not observe any hydration of this ion. For this reason, this ion exhibits high ion mobility.
The calculation of the geometry and energetics of hydrated protonated ions DMIP and DMTP isomers show that formation of hydronium ions with different grade of hydration is favourable. The differences in the degree of hydration of the of DMIP and DMTP ions are in large extent responsible for differences in their ion mobilities. They are ionized preferentially via s reaction (2).

Conclusions

We have studied APCI ionisation using $(H^+\cdot(H_2O)_{3,4})$ reactant ions to three isomers of DMP using IMS and IMS-oaTOF MS techniques. This study shows that APCI to these species is conformer selective. In the case of DMP molecule only DMP(III) conformer has PA higher than the RI and its ionisation results in $M\cdot H^+$ formation. The calculations support the experimental observation regarding weak hydration degree of this ion. The other conformers of DMP with PA lower than RI and the isomers DMIP and DMTP are ionised via adduct formation reactions resulting in formation of $M\cdot H^+\cdot(H_2O)$ ions. The differences in the structure of the ions and in the hydration degree result in significant differences in the ion mobilities of the molecules.

Conflicts of interest

There are no conflicts to declare.

Acknowledgements

This project has received funding from the European Union's Horizon 2020 research and innovation programme under the Marie Skłodowska-Curie grant agreement No 674911 and from the European Union's Horizon 2020 research and innovation programme under grant agreement No 692335. This work was supported by the Slovak Research and Development Agency (contract no. APVV-0259-12 and APVV-15-0580) and the Slovak Grant Agency for Science (contract no. VEGA 1/0733/17).

References

1 T. Schettler, 'Human exposure to phthalates via consumer products', International Journal of Andrology, vol. 29, no. 1, pp. 134–139, Feb. 2006.

2 A. Earls, I. Axford, and J. Braybrook, 'Gas chromatography–mass spectrometry determination of the migration of phthalate plasticizers from polyvinyl chloride toys and childcare articles', Journal of Chromatography A, vol. 983, no. 1–2, pp. 237–246, Jan. 2003.

3 R. A. Rudel and L. J. Perovich, 'Endocrine disrupting chemicals in indoor and outdoor air', Atmospheric Environment, vol. 43, no. 1, pp. 170–181, Jan. 2009.

4 R. Habert, V. Muczynski, A. Lehraiki, R. Lambrot, C. Leıcureuil, ´ C. Levacher, H. Coffigny, C. Pairault, D. Moison, R. Frydman, V. Rouiller-Fabre, Adverse effects of endocrine disruptors on the foetal testis development: focus on the phthalates, Histochem. Cytobiol. 47 (2009) 67–74

5 G. Latini, G. Knipp, A. Mantovani, M.L. Marcovecchio, F. Chiarelli, O. Soder, ¨Endocrine disruptors and human health, Mini-Rev. Med. Chem. 10 (2010) 846–855.

6 C. A. Staples, D. R. Peterson, T. F. Parkerton, and W. J. Adams, 'The environmental fate of phthalate esters: A literature review', Chemosphere, vol. 35, no. 4, pp. 667–749, Aug. 1997.

7 A. Paluselli, V. Fauvelle, N. Schmidt, F. Galgani, S. Net, and R. Sempéré, 'Distribution of phthalates in Marseille Bay (NW Mediterranean Sea)', Science of The Total Environment, vol. 621, pp. 578–587, Apr. 2018.

8 D. Kashyap and T. Agarwal, 'Concentration and factors affecting the distribution of phthalates in the air and dust: A global scenario', Science of The Total Environment, vol. 635, pp. 817–827, Sep. 2018.

9 J. Fischer, K. Ventura, B. Prokeš, and P. Jandera, 'Method for determination of plasticizers in industrial emissions', Chromatographia, vol. 37, no. 1–2, pp. 47–50, Jul. 1993.

10 J. H. Petersen and T. Breindahl, 'Plasticizers in total diet samples, baby food and infant formulae', Food Additives and Contaminants, vol. 17, no. 2, pp. 133–141, Feb. 2000.

11 M. J. Silva et al., 'Improved quantitative detection of 11 urinary phthalate metabolites in humans using liquid chromatography–atmospheric pressure chemical ionization tandem mass spectrometry', Journal of Chromatography B, vol. 789, no. 2, pp. 393–404, Jun. 2003.

12 M. Castillo, M. F. Alpendurada, and D. Barceló, 'Characterization of organic pollutants in industrial effluents using liquid chromatography-atmospheric pressure chemical ionization-mass spectrometry', Journal of Mass Spectrometry, vol. 32, no. 10, pp. 1100–1110, Nov. 1997.

13 M. Fernández-Amado, M. C. Prieto-Blanco, P. López-Mahía, S. Muniategui-Lorenzo, and D. Prada-Rodríguez, 'A comparative study of extractant and chromatographic phases for the rapid and sensitive determination of six phthalates in rainwater samples', Chemosphere, vol. 175, pp. 52–65, May 2017.

14 D. F. Hagen, 'Characterization of isomeric compounds by gas and plasma chromatography', Analytical Chemistry, vol. 51, no. 7, pp. 870–874, Jun. 1979.

15 E.J. Poziomek, and Gary A. Eiceman, Solid-phase enrichment, thermal desorption, and ion mobility spectrometry for field screening of organic pollutants in water, Environ. Sci. Technol., 1992, 26 (7), pp 1313–1318, July 1992

16 D. A. Barnett, R.W. Purves, B. Ells, R. Guevremont, Separation of o-, m- and p-phthalic acids by high-field asymmetric waveform ion mobility spectrometry (FAIMS) using mixed carrier gases, J. Mass Spectrometry, 2000, vol. 35 (8) pp 976-980, August 2000

17 A. J. Midey, A. Camacho, J. Sampathkumaran, C. A. Krueger, M. A. Osgood, and C. Wu, 'High-performance ion mobility spectrometry with direct electrospray ionization (ESI-HPIMS) for the detection of additives and contaminants in food', Analytica Chimica Acta, vol. 804, pp. 197–206, Dec. 2013.

18 C. Gobble, J. Chickos, and S. P. Verevkin, 'Vapor Pressures and Vaporization Enthalpies of a Series of Dialkyl Phthalates by Correlation Gas Chromatography', Journal of Chemical & Engineering Data, vol. 59, no. 4, pp. 1353–1365, Apr. 2014.

19 M. Sabo et al., 'Direct Liquid Sampling for Corona Discharge Ion Mobility Spectrometry', Analytical Chemistry, vol. 87, no. 14, pp. 7389–7394, Jul. 2015.

20 M. Sabo and S. Matejčík, 'A corona discharge atmospheric chemical ionization source with selective NO(+) formation and its application for monoaromatic VOC detection', Analyst, vol. 138, no. 22, pp. 6907-6912, Nov. 2013.

21 M. Sabo and Š. Matejčík, 'Corona Discharge Ion Mobility Spectrometry with Orthogonal Acceleration Time of Flight Mass Spectrometry for Monitoring of Volatile Organic Compounds', Analytical Chemistry, vol. 84, no. 12, pp. 5327–5334, Jun. 2012.

22 G. Eiceman, E. Nazarov, and J. Stone, 'Chemical standards in ion mobility spectrometry', Analytica Chimica Acta, vol. 493, no. 2, pp. 185–194, Oct. 2003.

23 H.-P. Cheng, "Water Clusters: Fascinating Hydrogen-Bonding Networks, Solvation Shell Structures, and Proton Motion," The Journal of Physical Chemistry A, vol. 102, no. 31, pp. 6201–6204, Jul. 1998.

24 E. P. L. Hunter and S. G. Lias, 'Evaluated Gas Phase Basicities and Proton Affinities of Molecules: An Update', Journal of Physical and Chemical Reference Data, vol. 27, no. 3, pp. 413–656, May 1998.

25 Gaussian 09, Revision C.01, M. J. Frisch, G. W. Trucks, H. B. Schlegel, G. E. Scuseria, M. A. Robb, J. R. Cheeseman, G. Scalmani, V. Barone, B. Mennucci, G. A. Petersson, H. Nakatsuji, M. Caricato, X. Li, H. P. Hratchian, A. F. Izmaylov, J. Bloino, G. Zheng, J. L. Sonnenberg, M. Hada, M. Ehara, K. Toyota, R. Fukuda, J. Hasegawa, M. Ishida, T. Nakajima, Y. Honda, O. Kitao, H. Nakai, T. Vreven, J. A. Montgomery, Jr., J. E. Peralta, F. Ogliaro, M. Bearpark, J. J. Heyd, E. Brothers, K. N. Kudin, V. N. Staroverov, T. Keith, R. Kobayashi, J. Normand, K. Raghavachari, A. Rendell, J. C. Burant, S. S. Iyengar, J. Tomasi, M. Cossi, N. Rega, J. M. Millam, M. Klene, J. E. Knox, J. B. Cross, V. Bakken, C. Adamo, J. Jaramillo, R. Gomperts, R. E. Stratmann, O. Yazyev, A. J. Austin, R. Cammi, C. Pomelli, J. W. Ochterski, R. L. Martin, K. Morokuma, V. G. Zakrzewski, G. A. Voth, P. Salvador, J. J. Dannenberg, S. Dapprich, A. D. Daniels, O. Farkas, J. B. Foresman, J. V. Ortiz, J. Cioslowski, and D. J. Fox, Gaussian, Inc., Wallingford CT, 2010.

26 Zhao, Y.; Truhlar, D. G. J. Phys. Chem. A 2006, 110, 10478−10486.

27 Zhao, Y.; Truhlar, D. G. Theor. Chem. Acc. 2008, 120, 215−241

28 J.-D. Chai and M. Head-Gordon, Phys. Chem. Chem. Phys., 10 (2008) 6615-20.

29 Lori A. Burns, Álvaro Vázquez-Mayagoitia, Bobby G. Sumpter, and C. David Sherrill, The Journal of Chemical Physics 134, 084107 (2011)

30 T. Wróblewski, L. Ziemczonek, and G. P. Karwasz, 'Proton transfer reactions for ionized water clusters', Czechoslovak Journal of Physics, vol. 54, no. S3, pp. C747–C752, Mar. 2004.

31 P. Kebarle, S. K. Searles, A. Zolla, J. Scarborough, and M. Arshadi, 'The solvation of the hydrogen ion by water molecules in the gas phase', J. Am. Chem. Soc., vol. 89, no. 25, pp. 6393-6399, Dec. 1967.